

In Situ X-ray Absorption Spectroscopy Investigation during the Formation of Colloidal Copper

J. Rothe,[†] J. Hormes,^{*,†} H. Bönemann,^{*,‡} W. Brijoux,[‡] and K. Siepen[‡]

Contribution from the Physikalisches Institut der Universität Bonn, Nussallee 12, D-53115 Bonn, Germany, and MPI für Kohlenforschung, Postfach 101353, D-45466 Mülheim/Ruhr, Germany

Received August 7, 1997. Revised Manuscript Received April 7, 1998

Abstract: The reduction of $[\text{N}(\text{octyl})_4]_2[\text{CuCl}_2\text{Br}_2]$ in organic solution (toluene) using $\text{Li}[\text{BEt}_3\text{H}]$ leads to colloidal Cu protected by cationic surfactants (NR_4^+). According to HRTEM (high-resolution transmission electron microscopy) and UV/vis data, the organosol is composed of relatively large Cu particles with diameters of between 5 and 10 nm. An in situ XANES (X-ray absorption near edge structure) investigation was performed for the first time during the colloid synthesis. Our measurements revealed the formation of an intermediate Cu^+ state prior to the nucleation of the particles, thus giving direct insight into the mechanism of the colloid formation. The significant differences between the near edge structures of the bulk sample and the colloidal Cu have to be traced back to structural disorder in the lattice of this nanosized material.

Introduction

For centuries the attraction of colloidal metals—especially gold sols—was primarily due to their intensive colors which enabled their application as pigments for the manufacturing of glass or ceramics. Today a rapidly growing number of applications (e.g., catalysis, metal ceramic composites¹) have emerged which are directly connected to the unique electronic structure of the nanosized metal particles or their extremely large specific surface area. When the transition from bulk metals to small particles or clusters with *mesoscopic* dimensions is considered, dramatic changes of all properties depending on the distribution of the free electrons are expected. Thus, the investigation of colloidal metals is also a topic of fundamental interest.

Recently, Bönemann et al. have shown that a large variety of transition elements belonging to the groups of coin and noble metals are accessible as colloidal dispersions in organic media (THF (tetrahydrofuran) or toluene) by reducing the corresponding halides with triethylhydroborate.^{2–5} The cationic tetraalkylammonium surfactant NR_4^+ , either as the counterion of the reducing agent triethylhydroborate or of the halogenometalate which should be reduced, serves as an organic coating which by means of steric stabilization is supposed to prevent the metal particles with diameters of a few nanometers from agglomeration.

The first observations made of colloidal metal dispersions concerned their sometimes intensive colors, resulting from a

strong absorption in the visible region of the spectrum. The shape and size as well as the surface composition of the colloidal metal particles determine the absorption characteristics in the ultraviolet and visible spectral region. Consequently, UV/vis spectroscopy is commonly used to characterize colloidal solutions and educt materials. The occurrence of characteristic absorption bands, explained by Mie's theory as the excitation of plasmon resonances,⁶ serves as a "fingerprint" for the complete transformation of the educt materials.

The initial steps in the synthesis of metal colloid particles through the chemical reduction of metal salts or metalates, with the formation of a zerovalent "seed" and the successive agglomeration and reduction of metal ions to build up metal clusters of growing nuclearity, are still a matter of speculation.

X-ray absorption spectroscopy (XAS)⁷ is especially suited as a tool for the investigation of metal (complex) compounds due to its unique ability for gaining a direct insight into the geometric and electronic structure of an absorbing metallic center. The technique has already proven to be a powerful tool for the investigation of transition metal colloids.^{8,9} In the following we describe our attempts to shed some light on the early steps of colloid formation by an in situ measurement using the energy dispersive (DEXAFS) technique.¹⁰ Considering the photon flux in the polychromatic focus of the energy dispersive monochromator (EDM) at ELSA as well as the concentration of the metal ions in the educt solution, the synthesis of the $\text{Cu}_{\text{colloid}}[\text{N}(\text{octyl})_4^+]\text{Br}^-$ dispersion in toluene was found to be a model system well suited for this investigation.

[†] Universität Bonn.

[‡] MPI für Kohlenforschung.

(1) Bradley, J. S. In *Clusters and Colloids: from Theory to Applications*; Schmid, G., Ed.; VCH: Weinheim, 1994.

(2) Bönemann, H.; Brijoux, W.; Richter, J.; Becker, R.; Hormes, J.; Rothe, J. *Z. Naturforsch. B* **1995**, *50* (3), 333–338.

(3) Bönemann, H.; Brijoux, W. In *Active Metals*; Firstner, A., Ed.; VCH: Weinheim 1996.

(4) Bönemann, H.; Brijoux, W.; Brinkmann, R.; Fretzen, R.; Jousen, T.; Kppler, R.; Korall, B.; Neiteler, P.; Richter, J. *J. Mol. Catal.* **1994**, *86*, 129–177.

(5) Bönemann, H.; Brijoux, W. In *Advanced Catalysts and Nanostructured Materials*; Moser, W. R., Ed.; Academic Press: New York, 1996.

(6) Creighton, J. A.; Eadon, D. G. *J. Chem. Soc., Faraday Trans.* **1991**, *87* (24), 3881–3891.

(7) Koningsberger, D. C.; Prins, R., Eds. *X-ray Absorption: Techniques of EXAFS, SEXAFS and XANES*; J. Wiley & Sons: New York, 1988.

(8) Rothe, J.; Franke, R.; Pollmann, J.; Hormes, J.; Bönemann, H.; Brijoux, W.; Siepen, K.; Richter, J. *Fresenius' J. Anal. Chem.* **1996**, *355*, 372–374.

(9) Franke, R.; Rothe, J.; Pollmann, J.; Hormes, J.; Bönemann, H.; Brijoux, W.; Hindenburg, Th. *J. Am. Chem. Soc.* **1996**, *118*, 12090–12097.

(10) Tolentino, H.; Dartyge, E.; Fontaine, A.; Tourillon, G. *J. Appl. Crystallogr.* **1988**, *21*, 15–21.

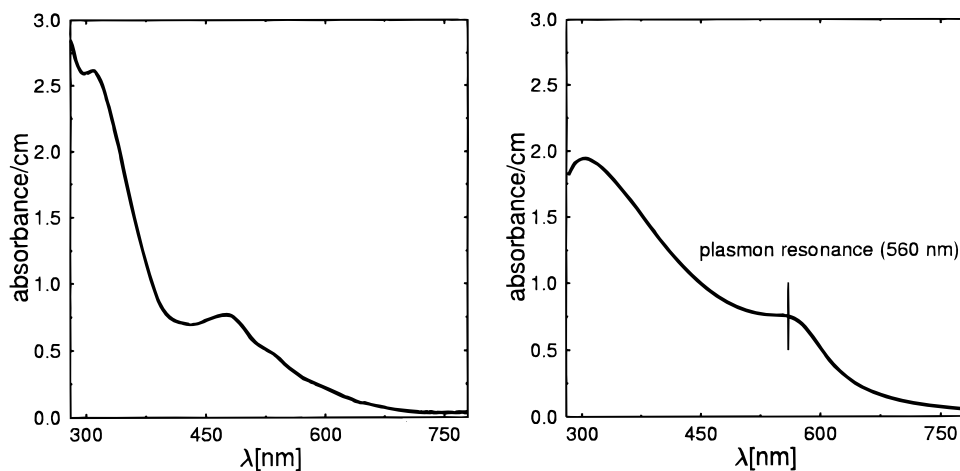


Figure 1. Left: UV/vis spectrum of $[N(\text{octyl})_4]_2[\text{CuCl}_2\text{Br}_2]$ in toluene. Right: UV/vis spectrum of colloidal Cu stabilized by $N(\text{octyl})_4^+$ in toluene. Note the plasmon resonance at 560 nm.

Experimental Section

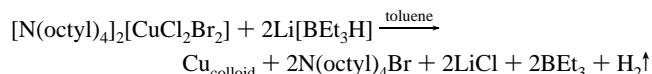
XANES Measurements. Cu K XANES measurements (Cu 1s binding energy 8979 eV) have been performed at the beamlines BN1 and BN3 of the synchrotron radiation laboratory at the Electron Stretcher and Accelerator ELSA¹¹ (Bonn University Institute of Physics) employing the energy dispersive as well as the standard transmission technique. For all measurements, ELSA was run at an electron energy of 2.3 GeV in storage ring mode and at an average current of 40 mA. The energy dispersive spectrometer¹² was equipped with a triangular cut Si(400) crystal ($2d = 2.715 \text{ \AA}$) which was cylindrically bent in order to focus a photon energy bandwidth ΔE of approximately 170 eV onto the sample at a distance of approximately 120 cm. A photodiode array (Reticon RL1024SAU) consisting of 1024 pixels was used as a position sensitive detector giving a resolution of 0.17 eV/step. This corresponds well to the minimum energy step width of 0.21 eV of the standard monochromator used in the sequential recording of absorption spectra. This one is a Lemonnier-type¹³ double-crystal monochromator equipped with a pair of plane Ge(422) crystals ($2d = 2.306 \text{ \AA}$). The agreement in resolution of both spectrometers has been confirmed by comparing the shape of the near edge absorption features of a $7.5 \mu\text{m}$ Cu foil measured with both techniques. This comparison is also required for the transformation of the position scale of the individual photodiodes to the energy scale of the absorption features. The standard X-ray absorption transmission measurements were performed using Ar-filled ionization chambers (200 mbar) detecting the primary and transmitted beam intensities. For the calibration of the energy scale of the monochromator, the Cu 1s energy was assigned to the first inflection point in the spectrum of the Cu foil (8979 eV). All reported XANES spectra are relative to this assignment.

To compare the measured absorption curves quantitatively, a linear background was fitted to the preedge region (8910–8960 eV) and then subtracted before subsequent normalization with respect to the “edge jump”. The edge height was determined as the average of the first EXAFS oscillations (i.e., the estimation of the atomic background between 9020 and 9100 eV).

A sample cell for the XAS measurements of liquids comparable to the one described in ref 14 was developed for the investigation of the colloidal solutions. Two stainless steel rings with an inner diameter of 12 mm are pressed by six screws onto both sides of Teflon distance rings of variable thickness to form a cylindrical block, while the sample volume is sealed by $12.5 \mu\text{m}$ Kapton windows. The enclosed volume

is accessible by canules of 0.5 mm diameter which fit into radial holes drilled in the Teflon ring. For measurements of air-sensitive liquids, these holes are sealed with needles before mounting of the cell into the measuring chamber. The reference compounds used were fcc-Cu metal foil ($7.5 \mu\text{m}$) as well as $\text{Cu}^{\text{II}}\text{O}$ and Cu_2O prepared as finely ground powders fixed on adhesive Kapton tape.

Preparation of the NR_4^+ -Stabilized Cu Colloid. The synthesis of the NR_4^+ -protected colloidal Cu by chemical reduction of the tetraoctylammonium halogenocuprate is carried out according to¹⁵



The cuprate is formed from suspended CuCl_2 (0.38 g, 2.79 mmol) and $N(\text{octyl})_4\text{Br}$ (3.05 g, 5.58 mmol) in 100 mL of toluene by ultrasonic irradiation at room temperature for 20 min. Under Ar atmosphere a stoichiometric amount of a 5.58 mmol solution of $\text{Li}[\text{BEt}_3\text{H}]$ is added to the dark red solution at 60°C over a 10 min period. The addition of the reducing agent initiates a rapid reaction visible by a color change of the solution from dark red to bright yellow, followed by a second color change to wine red after several minutes. When carrying out in situ XAS measurements with the energy dispersive monochromator, we used sealed glass flasks for storing the educt solution and the reducing agent under argon. The liquids were then injected into the sample cell using precision syringes. The sample cell (volume 0.9 mL) and the syringes were rinsed several times with Ar in order to avoid the decomposition of $\text{Li}[\text{BEt}_3\text{H}]$. After injection of the reducing agent, manual stirring ensured that the liquids were thoroughly mixed before the sample cell was mounted at the focal plane of the spectrometer. Despite cooling the steel block of the cell in a bath of liquid nitrogen and ethanol before filling, we have as yet not been successful in reducing the reaction rate of the initial step (formation of the yellow solution) which occurs instantaneously. Only when the reducing agent was added in excess—possibly due to the imperfect inert gas conditions which lead to the partial decomposition of $\text{Li}[\text{BEt}_3\text{H}]$ on air contact—the transformation of the intermediate yellow solution to the wine red colloidal dispersion was observed after several minutes. The UV/vis absorption of the educt (Figure 1, left) and the colloidal solution (Figure 1, right) serves as a “fingerprint” for the complete transformation of the Cu complex. The absorption maximum at 560 nm in Figure 1 (right) is characteristic of copper organosols containing metal particles with diameters of between 5 and 10 nm.¹⁵ Beginning with the intermediate state, XANES spectra were recorded every 60 s over a period of 30 min.

Results and Discussion

By comparing the Cu K near edge structure observed for a variety of mono- and divalent Cu compounds—e.g., in the case

(15) Hindenburg, Th. *Ph.D. Thesis*; RWTH Aachen, 1995.

(11) Althoff, K. H.; v. Drachenfels, W.; Dreist, A.; Husmann, D.; Neckening, M.; Nuhn, H. D.; Schauerte, W.; Schillo, M.; Schittko, F. J.; Wermelskirchen, C. *Part. Accel.* **1990**, 27, 101–106.

(12) Blank, H.; Neff, B.; Steil, S.; Hormes, J. *Rev. Sci. Instrum.* **1992**, 63 (1), 1334–1337.

(13) Lemonnier, M.; Collet, O.; Depautex, C.; Esteva, J. M.; Raoux, D. *Nucl. Instr. Methods* **1978**, 152, 109.

(14) Marcos, E. S.; Gil, M.; Martinez, J. M.; Muñoz-Paéz, A. M.; Marcos, A. *S. Rev. Sci. Instrum.* **1994**, 65 (6), 2153–2154.

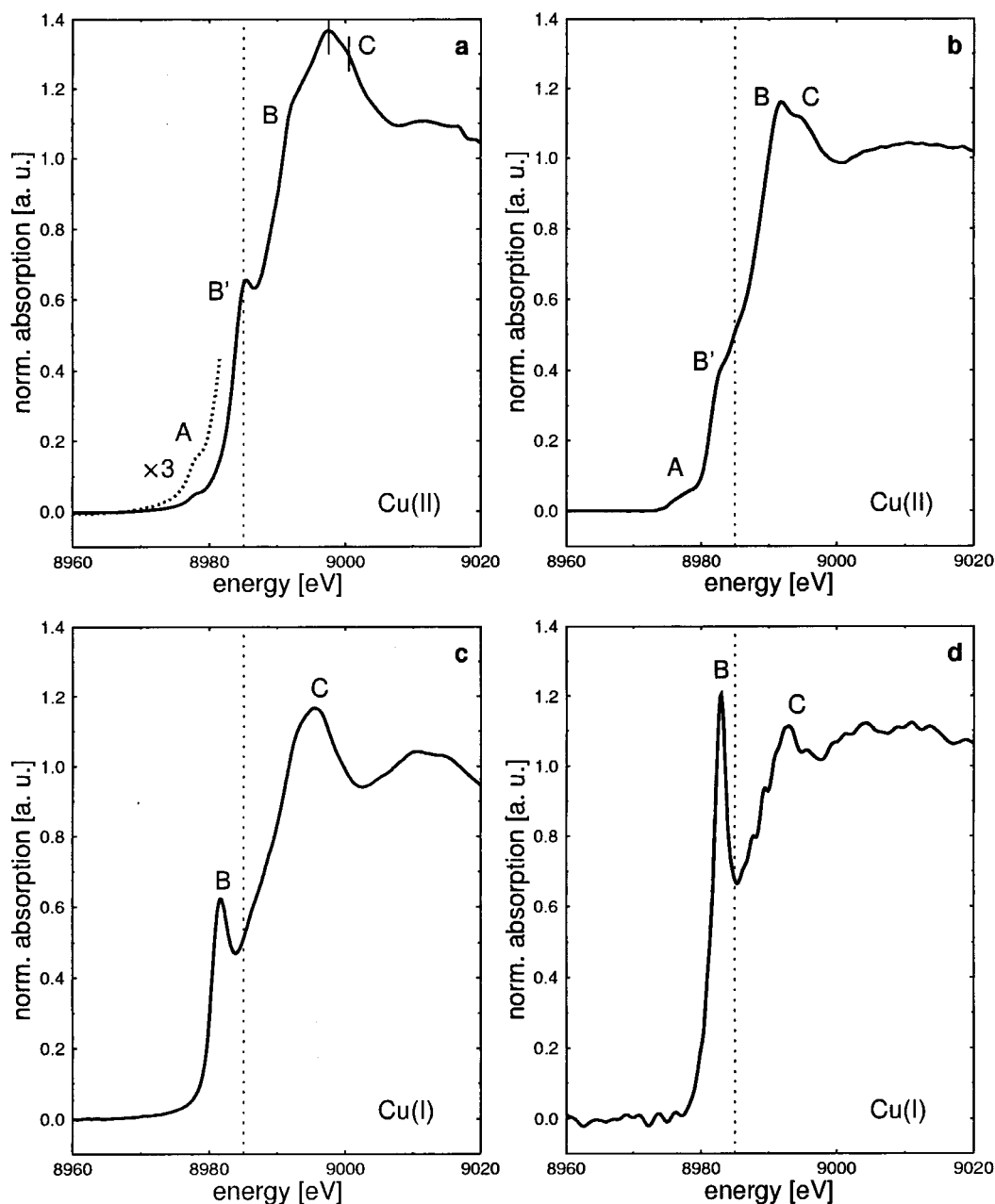


Figure 2. Cu K XANES: (a) CuO, (b) $[N(\text{octyl})_4]_2[\text{CuCl}_2\text{Br}_2]$ in toluene, (c) Cu_2O , (d) DEXAFS spectrum of the intermediate Cu^+ state after addition of $\text{Li}[\text{BEt}_3\text{H}]$. The vertical line marks 8985 eV.

of the investigation of the enzyme laccase by Kau et al.,¹⁶ the analysis of the role of Cu sites in ZnO methanol synthesis catalysts,¹⁷ or the characterization of the coordination geometry of Cu ions in zeolites¹⁸—it has been possible to postulate empirical rules for correlating XANES with both the electronic state of Cu ions and the geometry of their molecular surroundings. Usually Cu^{2+} complexes are characterized by tetragonal symmetries, i.e., square planar or square bipyramidal coordination of the metal ions (Figure 4a). As a consequence of a slight distortion of the coordination polyhedron caused by the Jahn–Teller effect, these complexes (valence electron configuration $3d^9$) display only an extremely weak $1s \rightarrow 3d$ (“preedge”) transition (peak A at 8979 eV in the XANES of CuO in Figure

2a). The resonances at higher energies within the rising edge (denoted as B, B', and C in Figure 2a) are to various degrees pronounced (in fact the structure C represents two transitions which are not resolved; see below), depending on the type of neighbor atoms and on the ionic character of the bonding between Cu and its ligands. A comprehensive description of these structures was given by Kosugi et al.¹⁹ based on the comparison of polarized Cu K XANES measurements on oriented single crystals and SCF (self-consistent field) calculations. The authors describe the resonances B and B' as due to $1s \rightarrow 4p_z$ transitions with and without LMCT (ligand to metal charge transfer), respectively. This LMCT is due to screening by the additional d electron, and hence the final state $1s^1 \dots 0.3d^{10}L^+4p^1$ is lowered relative to $1s^1 \dots 0.3d^94p^1$, where L^+ denotes a ligand with a missing valence electron. Accordingly, the resonance C at higher energy is ascribed to the $1s \rightarrow 4p_{x,y}$

(16) Kau, L.-S.; Spira-Solomon, D. J.; Penner-Hahn, J. E.; Hodgson, K. O.; Solomon, E. I. *J. Am. Chem. Soc.* **1987**, *109*, 6433–6442.

(17) Kau, L.-S.; Hodgson, K. O.; Solomon, E. I. *J. Am. Chem. Soc.* **1989**, *111*, 7103–7109.

(18) Yamashita, H.; Matsuoka, M.; Tsuji, K.; Shioya, Y.; Anpo, M.; Che, M. *J. Phys. Chem.* **1996**, *100*, 397–402.

(19) Kosugi, N.; Yokoyama, T.; Asakura, K.; Kuroda, H. *Chem. Phys.* **1984**, *91*, 249–256.

transitions in the plane of symmetry of these complexes with and without “shake down”. The Cu K XANES of CuO in Figure 2a at least indicates the corresponding doublet structure (vertical lines), which can be better observed in the derivated spectrum. In the tetragonal ligand field the presence of the four neighboring atoms in the $x-y$ plane is responsible for the higher energy level of the $p_{x,y}$ orbitals with respect to p_z . The Cu K XANES measurement of the educt compound $[\text{N}(\text{octyl})_4]_2[\text{CuCl}_2\text{Br}_2]$ in Figure 2b displays the characteristic structures of a divalent Cu complex. Considering the energy positions and the relative intensities of the resonances, the measurement is quite similar to the spectrum of divalent Cu in square planar $[\text{NEt}_4]_2\text{CuCl}_4$ depicted in ref 19.

The near edge fine structure of linearly 2-fold coordinated Cu^+ complexes is characterized by a sharp absorption resonance between 8980 and 8985 eV (peak B in Figure 2c,d; in the case of Cu_2O each Cu atom is linearly coordinated by two oxygens whereas O is tetrahedrally coordinated by four Cu atoms). Again the interpretation of these structures was possible on the basis of polarized Cu K XANES measurements. Accordingly, peak B represents the $1s \rightarrow 4p_{x,y}$ transition in the plane perpendicular to the symmetry axis of the complex, whereas peak C can be explained as a $1s \rightarrow 4p_z$ transition—shifted to higher energies due to the repulsive interaction of the ligand field along the z axis.¹⁶ In the case of Cu^+ compounds the closed 3d shell prevents the observation of a pronounced preedge resonance ($1s \rightarrow 3d$) as well as the occurrence of any shake down satellite which is characteristic for Cu^{2+} compounds. Considering the absorption features in Figure 2d as well as the spectra of Cu_2O and the reference spectra presented in the literature, the intermediate state (yellow solution after addition of the reducing agent) observed during the colloid synthesis can obviously be ascribed to a linearly coordinated Cu^+ complex. The decrease in intensity of resonance B observable in Figure 3 that follows the formation of the intermediate state is most likely due to the direct conversion of the Cu^+ species to colloidal Cu, while it is impossible—on the basis of these measurements—to detect evidence for further intermediates.

A selection of Cu K XANES measurements recorded with the DEXAFS spectrometer during the transformation of the intermediate state (yellow solution) to the $\text{N}(\text{octyl})_4^+$ -stabilized Cu colloid is presented in Figure 3. The significantly higher noise level of the measurements of Cu in toluene solution compared to the spectrum of the Cu foil (no. 9 in Figure 3) is attributed to the reduced area density ($1.5 \text{ mg of Cu/cm}^2$ vs 67 mg of Cu/cm^2) in these samples. On this basis the following model of the colloid formation may be proposed (Figure 4):

(1) Cu^{2+} ions which are surrounded by two Cl^- and two Br^- ions in square planar coordination can be assumed to serve as the starting point for the reaction; two tetraoctylammonium cations are required for charge compensation (a, corresponding to Figure 3, no. 1).

(2) Addition of the reducing agent $\text{Li}[\text{BET}_3\text{H}]$ initiates in a first step the reduction of divalent Cu to monovalent Cu in linear 2-fold coordination (b, Figure 3, no. 2).

(3) These complexes agglomerate to form Cu clusters of higher nuclearity; the formation of “Cu–Cu bonds” cannot be imagined without the participation of the diffuse Cu 4s orbitals which are unoccupied in Cu^+ , and hence this last step has to go along with the complete reduction of the Cu ions to metallic valency (Figure 3, nos. 3–7).

(4) When the reaction has been completed, only the surface atoms of the colloidal particles can be assumed to be in a nonzero valency state due to the interaction with the cationic

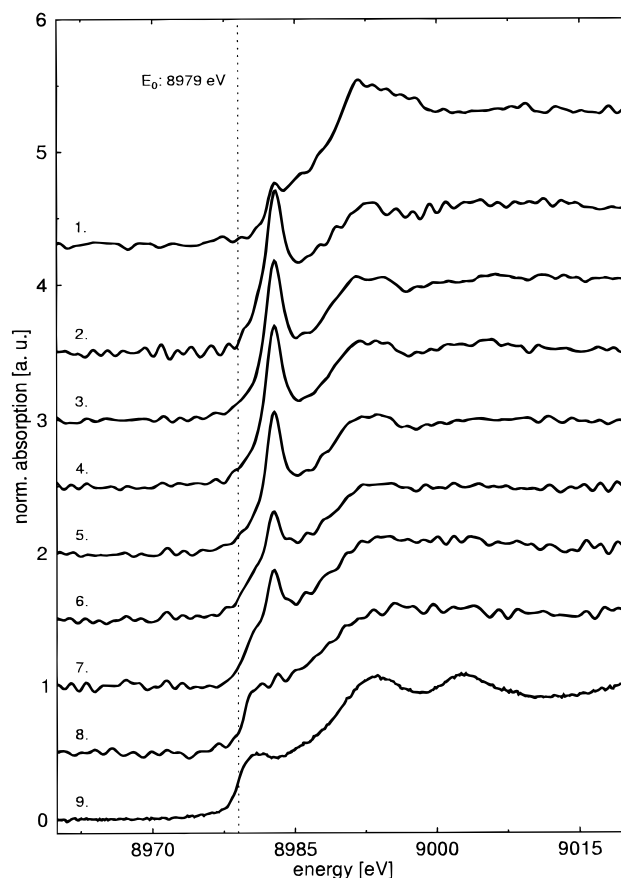


Figure 3. Cu K XANES. Synthesis of colloidal Cu stabilized by $\text{N}(\text{octyl})_4^+$: (1) $[\text{N}(\text{octyl})_4]_2[\text{CuCl}_2\text{Br}_2]$, (2) intermediate Cu^+ state, (3–7) cluster growth (~ 2 min between two spectra), (8) colloidal Cu (see also Figure 5), (9) fcc-Cu foil.

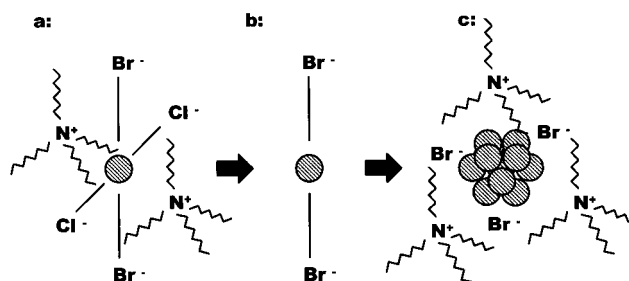


Figure 4. Proposed steps of the colloid formation: (a) divalent complex compound, (b) monovalent intermediate state, (c) $\text{N}(\text{octyl})_4^+$ -protected colloid particle (schematic).

surfactants or the bromide counterions (c, Figure 3, no. 8). In Figure 5 the Cu K XANES spectra of the final product of the reaction shown in Figure 3 and the fcc-Cu foil as recorded by sequential scanning with the double-crystal monochromator are compared, and the first derivatives of the spectra are plotted as an inset. The position of the first inflection point (which can be attributed to the position of the Fermi level in metallic systems) coincides, and the absorption features (note especially the $1s \rightarrow 3d$ transition always observed as a shoulder or distinct peak at the rising edge of the first-row transition metals²⁰) are similar. This is a strong indication of the predominant metallic character of Cu in the colloidal dispersion. Furthermore, the similarity between our colloid spectrum and the measurements performed by Montano et al.²¹ on “naked” Cu clusters embedded

(20) Agarwal, B. K. *X-ray Spectroscopy*; Springer Series in Optical Sciences 15; Springer: Berlin, Heidelberg, 1991.

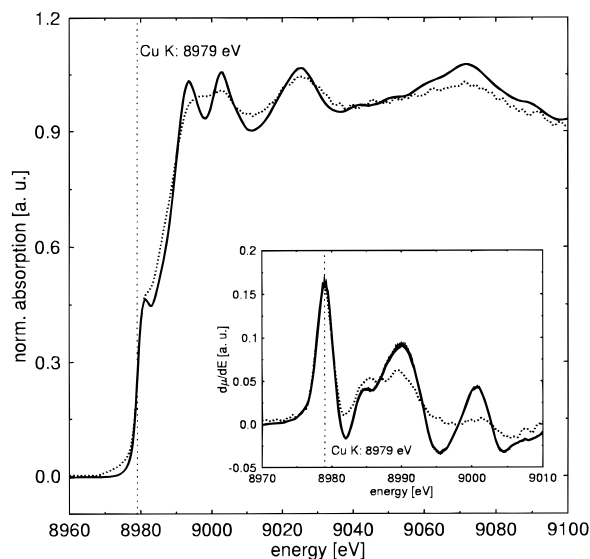


Figure 5. Cu K XANES: colloidal Cu in toluene (dots) and Cu bulk (solid line). The first derivative spectra are shown in the inset.

in a matrix of solid argon is remarkable. In their work the authors trace back the “smeared” appearance of the characteristic fine structure—especially of the double peak at the crest of the rising edge—to the absence of the fourth and higher coordination shells in their particles (average diameter 10 Å). This interpretation agrees with the results of multiple scattering calculations performed by Greaves et al.,²² whereas our own simulation using the FEFF6 program code by Rehr et al.²³ already showed the main features of the Cu bulk spectrum when the third shell in a regular fcc structure had been added.²⁴ In the case of colloidal Cu in toluene, we did not detect a shift of the absorption edge to higher energies in comparison with the bulk measurement as observed by Montano et al. (ca. 1.4 eV). This shift can be assumed to be caused by a “particle size effect”²⁵ or by the interaction with the host matrix. The results of the TEM (transmission electron microscopy) investigation of the

dried organosol in addition to the already mentioned UV/vis spectroscopic results strongly oppose the assumption of extremely small particles; they indicate a particle size between 5 and 10 nm. Consequently, the damping of the XANES features has to be attributed to the high degree of structural and/or thermal disorder of the lattice which is still significant in particles of this size.^{26,27}

Conclusions

The Cu K XANES investigation of the mechanism of the formation of colloidal Cu protected by $N(\text{octyl})_4^+$ in toluene via the chemical reduction of a Cu^{2+} complex yields evidence for the presence of an intermediate state which—by means of comparison to model compounds—can be ascribed to a linearly 2-fold coordinated Cu^+ species. The growth of clusters of zerovalent Cu atoms by agglomeration and the complete reduction of the intermediate compound has been shown to be a rather slow process in contrast to the initial step. The recorded near edge structures observed by excitation of the 1s electron into the lowest unoccupied electronic levels represent the free density of states associated with the absorber. Thus, comparison of our Cu K XANES measurements of a fcc-Cu foil and the colloid sample leads to the assumption that the band structure of the nanosized particles has not been completely developed. Distortions of the lattice of the Cu particles as a consequence of the surface tension or through the interaction with the coating shell of organic molecules—rather than the particle size—are likely to be responsible for this effect. Similar observations have been made at the Pt L_{III} edge in the case of NR_4^+ -coated Pt particles (2–3 nm diameter).²⁴ To obtain more detailed information on the structure of the Cu colloid and the influence of thermal disorder on the spectra, measurements at low temperatures as well as the performance of an EXAFS analysis would be of great importance.

Acknowledgment. We gratefully acknowledge the financial support by the BMBF, Bonn, under Contract No. 03 D 0007 A2, Dr. W. Wittholt for the preparation of the colloid samples, Dr. B. Tesche and Dipl.-Ing. B. Spliethoff (MPI für Kohlenforschung) for high-resolution transmission micrographs, and Dr. M. Pantelouris for reading the manuscript.

JA972748W

(21) Montano, P. A.; Shenoy, G. K.; Alp, E. E.; Schulze, W.; Urban, J. *Phys. Rev. Lett.* **1986**, *56* (19), 2076–2079.

(22) Greaves, G. N.; Durham, P. J.; Diakun, G.; Quinn, P. *Nature* **1981**, *294*, 139.

(23) Mustre de Leon, J.; Rehr, J. J.; Zabinsky, S. I.; Albers, R. C. *Phys. Rev. B* **1991**, *44*, 4146–4156.

(24) Rothe, J. *Ph.D. Thesis*; Bonn University, 1997; BONN-IR-97-05.

(25) Mason, M. G. *Phys. Rev. B* **1983**, *27* (2), 748–762.

(26) Clausen, B. S.; Topsoe, H. *Jpn. J. Appl. Phys.* **1993**, *32*, 95–98.

(27) Di Cicco, A.; Berrettoni, M.; Stizza, S.; Bonetti, E. *Physica B* **1995**, *208*, 209, 547–548.